

Constraints on color-flavored locked quark matter in view of the HESS J1731-347 event

K. Kourmpetis^{1,2},* P. Laskos-Patkos¹,† and Ch.C. Moustakidis¹‡

¹*Department of Theoretical Physics, Aristotle University of Thessaloniki, 54124 Thessaloniki, Greece*

²*Department of Physics, Eberhard Karl University of Tübingen, 72074 Tübingen, Germany*

Understanding the processes within compact stars hinges on astrophysical observations. A recent study reported on the central object in the HESS J1731-347 supernova remnant (SNR), estimating a mass of $M = 0.77_{-0.17}^{+0.20} M_{\odot}$ and a radius of $R = 10.40_{-0.78}^{+0.86}$ km, making it the lightest neutron star ever observed. Conventional models suggest that neutron stars form with a minimum gravitational mass of about $1.17M_{\odot}$, raising the question: is this object a typical neutron star, or could it be our first encounter with an "exotic" star? To explore this, we employ the Color-Flavored Locked (CFL) equation of state (EoS), aiming to constrain it by integrating data from the HESS J1731-347 event with pulsar observations and gravitational wave detections. Additionally, we model hybrid EoS by combining the MDI-APR1 (hadronic) and CFL (quark) EoS, incorporating phase transitions via Maxwell construction. Our analysis indicates that CFL quark matter adequately explains all measurements, including the central compact object of HESS J1731-347. In contrast, hybrid models featuring CFL quark phases fail to account for the masses of the most massive observed pulsars.

Keywords: Neutron stars, Quark stars, Color-flavored locked matter, Hybrid stars, Equation of state

I. INTRODUCTION

The study of the equation of state of nuclear matter plays a pivotal role in understanding the fundamental properties of compact stars. These exotic objects, characterized by extreme densities and pressures, provide a unique laboratory for probing the behavior of matter under intense conditions [1–4]. The recent HESS J1731-347 event [5], a central compact object (CCO: isolated, radio quiet, non-accreting, thermally emitting neutron star found at the centres of SNR [6–8]) with an unusually low mass, has sparked renewed interest in exploring alternative forms of matter beyond traditional neutron stars. This intriguing discovery challenges our current understanding and opens the door to new possibilities in the study of dense matter physics.

The nature of the HESS J1731-347 CCO poses a strong theoretical challenge as up to this moment it is not clear how such light neutron stars could be produced in supernova explosions [9]. The peculiar characteristics of this compact object may suggest that neutron matter alone may not be sufficient to explain the observed properties, necessitating the consideration of more exotic forms of matter. Quark stars, composed of deconfined quarks, and hybrid stars, featuring a core of quark matter surrounded by a mantle of neutron matter, represent viable alternatives that must be investigated to fully understand the implications of this object. Brodie and Haber further emphasized that pure nuclear matter alone may be insufficient to account for the HESS J1731-347 CCO, whereas quark and hybrid models provide more accurate predictions [10].

In this work, we follow the proposal by Di Clemente *et al.* [11] and Horvath *et al.* [12], considering the compact central object (CCO) in HESS J1731-347 to be a quark strange star (SS). Strange stars are hypothetical compact objects made of strange quark matter (SQM), a type of quark matter that includes strange quarks, and are considered possible entities in the universe [13–18]. Strange quark matter is considered a strong candidate for the true ground state of matter [19–23]. As SQM, we employ the Color-Flavor Locked (CFL) model. At asymptotically high densities, surpassing nuclear density, where quark masses are negligibly small compared to the quark chemical potential, quark matter will enter a color-superconducting phase known as the Color-Flavor-Locked (CFL) state [24–27], where quarks of different colors and flavors form Cooper pairs [28, 29]. The CFL matter, also suggested in Ref. [30], could potentially explain the nature of the object observed in the HESS J1731-347 SNR.

In scenarios where the quark phase is not absolutely stable but emerges as the dominant phase at sufficiently high densities, hybrid stars are formed [31–35]. In the present work, we construct a hybrid model that combines the MDI-APR1 EoS [36] with CFL matter, featuring a Maxwell phase transition [2]. Hybrid matter is also considered a strong candidate for the nature of the HESS J1731-347 CCO [10, 37–41].

Naturally, it is essential that any proposed EoS not only explains the HESS J1731-347 event but also aligns with the broader body of observational data. The physics governing the structure of compact stars should be universal, implying that any EoS must be applicable across a range of observations, including those of more massive pulsars [42–44] and the GW170817 merging event [45]. Clearly, any EoS must also adhere to fundamental compactness constraints, including the black hole limit [46], the Buchdahl limit [47], and the causality limit [48].

* kkourmpe@physics.auth.gr

† plaskos@physics.auth.gr

‡ moustaki@auth.gr

The motivation behind this study is to impose advanced and precise constraints on the Bag Constant and Superconducting Gap parameter space within the CFL EoS. By exploring various combinations of these parameters, we aim to identify the specific value pairs that not only predict the existence of the HESS J1731-347 CCO, but also accurately describe the properties of the GW170817 event and the most massive known pulsars. Additionally, we investigate the potential of a hybrid model, to determine whether a CFL hybrid model can provide a viable explanation for the formation and properties of all these objects. The findings will contribute to our understanding of the dense matter EoS and may offer new insights into the possible existence of quark and hybrid stars. Furthermore, this work underscores the importance of consistency between theoretical models and observational data as we seek to connect the macroscopic parameters of a star (mass and radius) observed with its microscopic properties (e.g. Δ), dictated by theory.

This paper is organized as follows: in section II, we present the theoretical model utilized in this study. The section III provides the results for each model and a detailed discussion of these findings. Finally, in section IV, we summarize the key insights and conclusions drawn from this work.

II. THE MODEL

A. TOV Equations

The structure of neutron stars is encapsulated in the so-called TOV equations, named after Tolman, Oppenheimer and Volkov [49]. These equations represent the generalization of Newtonian gravity to the domain of general relativity. The TOV equations are given by [50]:

$$\frac{dP(r)}{dr} = -\frac{GM(r)\rho(r)}{r^2} \left(1 + \frac{P(r)}{\rho(r)c^2}\right) \quad (1)$$

$$\left(1 + \frac{4\pi r^3 P(r)}{c^2 M(r)}\right) \left(1 - \frac{2GM(r)}{c^2 r}\right)^{-1}$$

$$\frac{dM(r)}{dr} = 4\pi r^2 \rho(r), \quad (2)$$

where $\rho(r) = \varepsilon(r)/c^2$ is the matter density and $\varepsilon(r)$ is the energy density. The solution of the system involves the transformation of the TOV equations, tailoring them to ensure their compatibility with numerical integration techniques [51].

B. Color-Flavored-Locked Equation of State

The EoS for CFL quark matter can be derived in the MIT bag model framework [52]. To the order of Δ^2 and m_s^2 (m_s represents the mass of the strange quark and μ

the chemical potential) the pressure and energy density can be expressed as follows ($\hbar = c = 1$) [27]:

$$P = \frac{3\mu^4}{4\pi^2} + \frac{9\alpha\mu^2}{2\pi^2} - B \quad (3)$$

$$\varepsilon = \frac{9\mu^4}{4\pi^2} + \frac{9\alpha\mu^2}{2\pi^2} + B \quad (4)$$

where,

$$\alpha = -\frac{m_s^2}{6} + \frac{2\Delta^2}{3} \quad (5)$$

Combining the above equations one can obtain an analytic expression for $\varepsilon(P)$ and $P(\varepsilon)$:

$$\varepsilon = 3P + 4B - \frac{9\alpha\mu^2}{\pi^2} \quad (6)$$

$$\text{where, } \mu^2 = -3\alpha + \left[\frac{4}{3}\pi^2(B + P) + 9\alpha^2\right]^{1/2} \quad (7)$$

$$P = \frac{\varepsilon}{3} - \frac{4B}{3} + \frac{3\alpha\mu^2}{\pi^2} \quad (8)$$

$$\text{where, } \mu^2 = -\alpha + \left[\alpha^2 + \frac{4}{9}\pi^2(\varepsilon - B)\right]^{1/2} \quad (9)$$

For CFL quark matter to be absolutely stable, its energy per baryon must be lower than the neutron mass (m_n) at zero pressure ($P = 0$) and temperature ($T = 0$) [18]. Consequently, the following condition must be met [27]:

$$\left.\frac{\varepsilon}{n_B}\right|_{P=0} = 3\mu \leq m_n = 939 \text{ MeV} \quad (10)$$

This result directly follows from the shared Fermi momentum among the three quark flavors in CFL matter, valid at $T = 0$ without any approximation. Since this condition must be satisfied at zero pressure, using Eq. 6, we have [53]:

$$B < -\frac{m_s^2 m_n^2}{12\pi^2} + \frac{\Delta^2 m_n^2}{3\pi^2} + \frac{m_n^4}{108\pi^2} \quad (11)$$

This equation defines a region in the $m_s - B$ plane where the energy per baryon is less than m_n for a specified value of Δ [53]. This condition combined with the constrain that two-flavoured quark matter should be less stable than nuclear matter, or $B \geq 57 \text{ MeV} \cdot \text{fm}^{-3}$ [18] in the MIT Bag Model framework, describe the so-called stability windows [53, 54].

C. Phase Transition: Maxwell Construction

In this work on hybrid stars, we combine neutron matter models with quark matter in the CFL phase to develop hybrid star equations of state. For the neutron phase, we adopt the MDI-APR1 EoS. The hadron to

quark phase transition is treated as a first-order phase transition using the Maxwell construction. This transition occurs at a constant pressure, accompanied by a discontinuity in energy density. Thermodynamic equilibrium between the two phases—phase I (hadronic) and phase II (quark)—is established when [2]:

$$P_I(\mu_B^I) = P_{II}(\mu_B^I) \quad \text{with} \quad \mu_B^I = \mu_B^{II}, \quad (12)$$

where P is the pressure and μ_B is the baryon chemical potential of each phase. Note that the condition for thermal equilibrium is trivially satisfied due to the use of zero temperature EoS.

III. RESULTS AND DISCUSSION

A. Pure CFL Quark Matter

In our analysis, we employ the expression that defines the CFL stability windows (Eq. (11)) while maintaining the mass of the strange quark constant at $m_s = 95$ MeV. Consequently, the relationship becomes a function within the $B - \Delta$ space. This function is plotted combined with the Bag Constant constraint resulting in a new stability window, as illustrated in Figure 1. The CFL equations of state used in this work are presented in Table I and they all reside within this stability window. For the CFL models utilized, we have used typical B and Δ values (B typical values are $\sim 57 - 150$ MeV \cdot fm $^{-3}$ and Δ values are $\sim 50 - 150$ MeV).

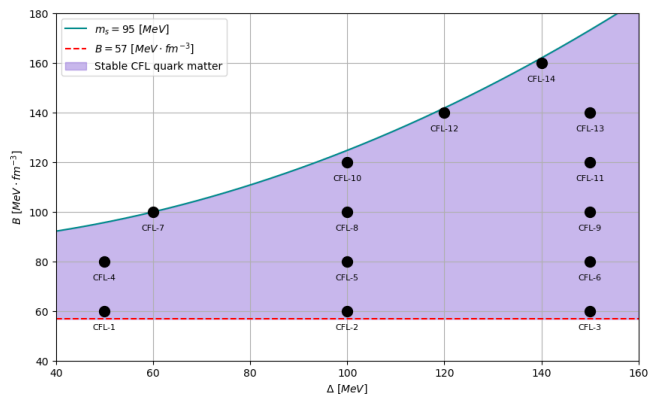


FIG. 1. CFL stability window for $m_s = 95$ MeV, including the CFL EoS employed. The red dashed line is the minimum value of B ($B \geq 57$). The coloured area indicates the range of B and Δ , for the given m_s value, where the CFL EoS is stable.

Having examined the stability of the CFL matter, we proceed by constructing the M-R diagram for the CFL EoS models listed in Table I. This graph is shown in Figure 2. Interestingly, the softest equations of state (those with the lowest maximum masses) are those closest to the $m_s = 95$ MeV curve in the $B - \Delta$ space, as depicted in Figure 1 (CFL-7, CFL-10, CFL-12, CFL-14). This

Model	B (MeV \cdot fm $^{-3}$)	Δ (MeV)
CFL-1	60	50
CFL-2	60	100
CFL-3	60	150
CFL-4	80	50
CFL-5	80	100
CFL-6	80	150
CFL-7	100	60
CFL-8	100	100
CFL-9	100	150
CFL-10	120	100
CFL-11	120	150
CFL-12	140	120
CFL-13	140	150
CFL-14	160	140

TABLE I. CFL EoS employed.

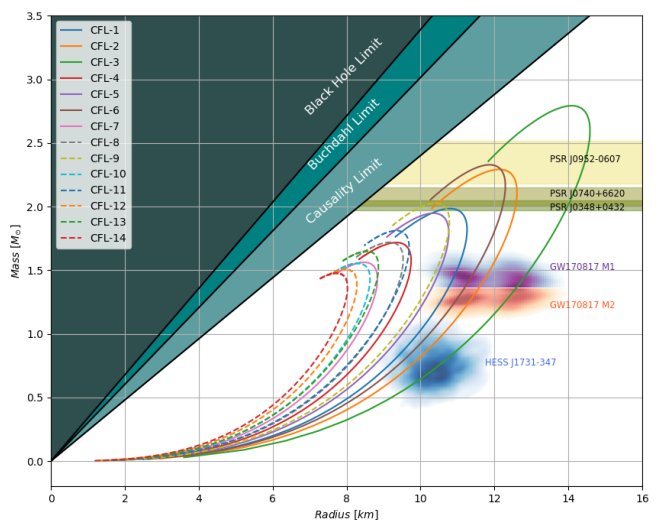


FIG. 2. M-R diagram for the CFL EoS presented in Table I. The graph includes constraints forced by pulsar observations (PSR J0348+0432, PSR J0740+6620, PSR J0952-0607), the GW170817 merging event and the CCO in the HESS J1731-347 SNR [5, 42–45].

observation aligns with the CFL stiffness dependence, as increasing the B parameter results in a softer EoS, and the $m_s = 95$ MeV curve represents the maximum B value for each Δ . On the other hand, the stiffest (those with the highest maximum masses) EoS are CFL-3, CFL-6 and CFL-2, all characterized by small B and high Δ values. We now examine the curves that satisfy all the criteria, including the strictest one imposed by the heaviest pulsar, PSR J0952-0607, under the hypothesis that it represents the upper mass limit for compact stars. It is evident that the EoS models that meet all the requirements are CFL-2 and CFL-6. Both of these share an analogous relationship between B and Δ values, with B

being 50-60% of Δ . The next stiffest EoS is CFL-3. Although it intersects the GW170817 and HESS J1731-347 regions, its maximum mass significantly exceeds that of the heaviest pulsar, with B being 40% of Δ . Conversely, the next softest EoS is CFL-9, which does not reach the heaviest pulsar range and has B at 67% of Δ . Therefore, to fulfill all criteria, the CFL EoS must have B approximately 50-60% of Δ , for typical B and Δ values. In order to be within these typical values, B should vary between 57 and ~ 80 $\text{MeV} \cdot \text{fm}^{-3}$. This is clearly illustrated in Figure 3, where we have plotted the M-R diagram for B values of 50% Δ and 60% Δ , showing that all the curves pass through all the constraints imposed by observations.

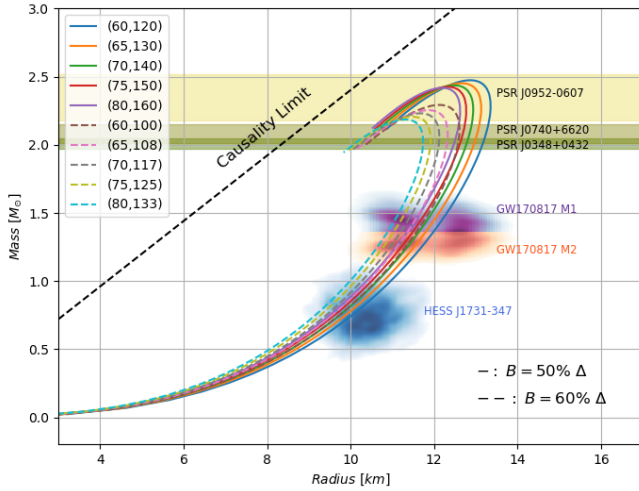


FIG. 3. M-R diagram that align with pulsar, gravitational wave and SNR CCO observations for CFL EoS. The solid line represents the EoS with $B = 0.5\Delta$, while the dashed ones the EoS with $B = 0.6\Delta$. The legend is in the form of $(B$ in $\text{MeV} \cdot \text{fm}^{-3}$, Δ in MeV).

We continue our analysis by generating M-R curves for a range of B and Δ values, assigning them typical values, and identify which of them align with all aforementioned measurements. This is illustrated in the contour plot in Figure 4. The area of interest is the greenish region, where all three events are predicted for B and Δ values around $57 - 85$ $\text{MeV} \cdot \text{fm}^{-3}$ and $75 - 150$ MeV , respectively. Both lower and upper boundaries of the greenish area, represented by the blue and red fit respectively, follow an almost linear function. The graph also accounts for the minimum value of the Bag Constant, constraining the $B - \Delta$ pairs inside a quadrilateral (considering the aforementioned typical values). This more accurate result is not far from the B and Δ analogy we roughly estimated in our previous analysis, as seen from the orange contour of Figure 4.

Lastly, we present the sound speed-pressure diagram for the CFL EoS in Figure 5. CFL matter adheres to the causality limit, with sound speed consistently below $c_s = 1$ and asymptotically approaching the conformal limit of $c_s^2 = 1/3$, as also noted by Flores and Lugones [53].

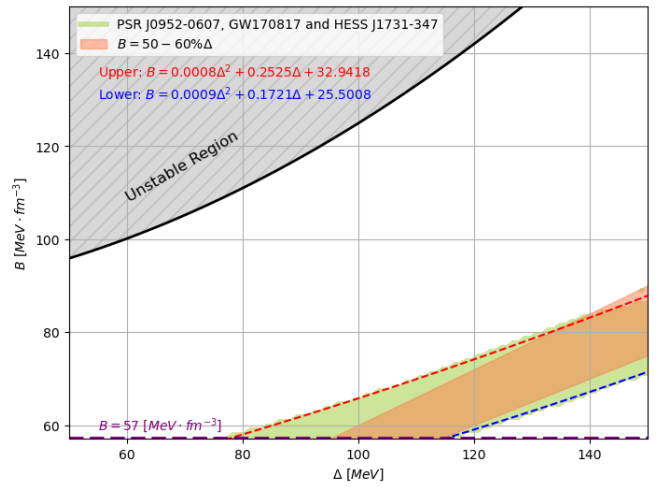


FIG. 4. Contours in the $B - \Delta$ plane. The greenish contour, formed by the two fits (red and blue) and the B_{min} (purple), represents $B - \Delta$ pair combinations that produce M-R curves that align with the PSR J0952-0607, GW170817 and HESS J1731-347 SNR observation. The orange region represents the previous constrain from Figure 3. The shaded region marks the unstable area.

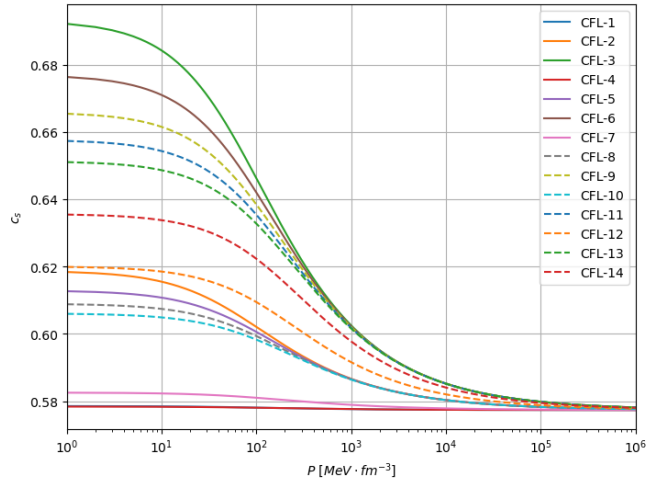
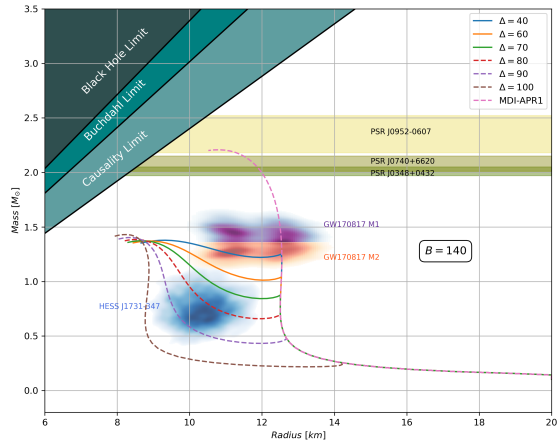


FIG. 5. $c_s - P$ diagram for the CFL models utilized. CFL matter respects causality and asymptotically reaches the ultra-relativistic limit in the high pressure regime.

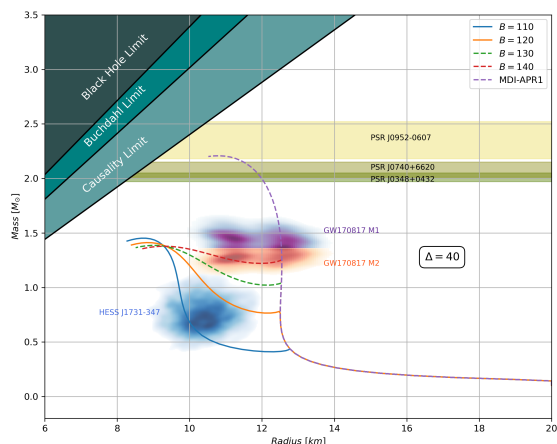
B. Hybrid CFL Matter

In Figure 6, we present the mass-radius diagrams for the hybrid CFL EoS constructed, considering two distinct cases: a) $B = 140$ and b) $\Delta = 40$, while varying the other parameter in each scenario. It is important to note that the selected $B - \Delta$ combinations fall outside the stability window shown in Figure 1. This is critical, as meta-stable states are required; otherwise, pure CFL matter would be energetically favored over the hybrid configuration.

The results indicate that the models are capable of re-



(a)



(b)

FIG. 6. M-R diagrams for the constructed hybrid models are presented for (a) varying Δ and a fixed $B = 140$ and for (b) varying B and a fixed $\Delta = 40$ (B in $\text{MeV} \cdot \text{fm}^{-3}$, Δ in MeV).

producing the HESS J1731-347 event via a hybrid branch of the hadronic EoS, which initiates between 0.5 and $1M_{\odot}$. However, the phase transition introduces a soft-

ening in the EoS, causing the maximum masses to fall well below $2M_{\odot}$. This discrepancy suggests that while the models can account for the HESS J1731-347 event, they are not consistent with other measurements, necessitating further refinement and alternative approaches.

IV. CONCLUSIONS

In this study, we conduct a comprehensive analysis of the CFL quark matter EoS, constraining its parameters to align with recent observations of the HESS J1731-347 CCO, as well as the GW170817 event and the heaviest known pulsar, PSR J0952-0607. Our results suggest that CFL quark matter is capable of explaining all the previously mentioned measurements, within a parameter space defined by $B \approx 50 - 60\% \Delta$, as a first approximation. This parameter range closely aligns with the formal constraints we derived, which are illustrated in Figure 4. Within this parameter window, pure CFL matter satisfies all observational criteria, while also respecting causality constraints. Therefore, CFL quark matter could be a promising candidate for the HESS J1731-347 CCO.

However, in the case of the hybrid CFL models developed, we find that although a hybrid branch can indeed reproduce the extremely low-mass HESS J1731-347 event, the maximum masses predicted by this model fall significantly below those observed for the most massive pulsars. A potential solution to this issue could involve incorporating a density-dependent Bag parameter, which decreases at higher densities, thereby stiffening the EoS, as suggested in Ref. [41]. While the exact nature of this object remains uncertain, ongoing research, coupled with advances in observational techniques, will be pivotal in resolving this enigmatic problem.

ACKNOWLEDGEMENTS

The authors thank Mr. Stefanos Kargas for his valuable assistance with the computational part of this study. The research work was supported by the Hellenic Foundation for Research and Innovation (HFRI) under the 5th Call for HFRI PhD Fellowships (Fellowship Number: 19175).

[1] N. K. Glendenning, *Compact Stars—Nuclear Physics, Particle Physics and General Relativity* (Springer, New York, 1997).
 [2] J. Schaffner-Bielich, *Compact Star Physics* (Cambridge University Press, Goethe University Frankfurt, 2020).
 [3] F. Weber, *Pulsars as Astrophysical Laboratories for Nuclear and Particle Physics* (Institute of Physics, Bristol, England, 1999).

[4] P. Haensel and A. Y. Potekhin and D. G. Yakovlev, *Neutron Stars 1: Equation of State and Structure* (Springer-Verlag, New York, 2007).
 [5] V. Doroshenko et al., *A strangely light neutron star within a supernova remnant*, *Nat. Astron.* **6**, 1444 (2023).
 [6] G.G. Pavlov, V.E. Zavlin, and D. Sanwal, *Thermal Radiation from Neutron Stars: Chandra Results*, Becker, W., Lesch, H., Trümper, J. (eds.) *Neutron Stars, Pulsars, and Supernova Remnants*, p. 273 (2002).

- [7] Pavlov G.G., Sanwal D., and Teter M.A., *Central Compact Objects in Supernova Remnants*, Camilo, F., Gaensler, B.M. (eds.) *Young Neutron Stars and Their Environments*, vol. 218, p. 239 (2004).
- [8] De Luca A., *Central compact objects in supernova remnants*, *J. Phys.: Conf. Ser.* **932**, 012006 (2017).
- [9] Y. Suwa et al., *On the minimum mass of neutron stars*, *Monthly Notices of the Royal Astronomical Society* **481**, 3305 (2018).
- [10] L. Brodie and A. Haber, *Nuclear and hybrid equations of state in light of the low-mass compact star in HESS J1731-347*, *Phys. Rev. C* **108**, 025806 (2023).
- [11] F. Di Clemente et al., *Is the compact object associated with HESS J1731-347 a strange quark star?*, [arXiv:2211.07485](https://arxiv.org/abs/2211.07485) (2024).
- [12] J. E. Horvath et al., *A light strange star in the remnant HESS J1731-347: Minimal consistency checks*, *A&A* **672**, L11 (2023).
- [13] C. Alcock, E. Farhi, and A. Olinto, *Strange Stars*, *ApJ* **310**, 261 (1986).
- [14] C. Alcock and A. V. Olinto, *Exotic Phases of Hadronic Matter and their Astrophysical Application*, *Ann. Rev. Nucl. Part. Sci.* **38**, 161 (1988).
- [15] P. Haensel, J. L. Zdunik, and R. Schaefer, *Strange quark stars*, *A&A* **160**, 121 (1986).
- [16] J. Madsen, *Physics and astrophysics of strange quark matter*, *Lect. Notes Phys.* **516**, 162 (1999).
- [17] F. Weber, *Strange quark matter and compact stars*, *Prog. Part. Nucl. Phys.* **54**, 193 (2005).
- [18] E. Farhi and R. L. Jaffe, *Strange matter*, *Phys. Rev. D* **30**, 2379 (1984).
- [19] N. Itoh, *Hydrostatic Equilibrium of Hypothetical Quark Stars*, *Prog. Theor. Phys.* **44**, 291 (1970).
- [20] A. R. Bodmer, *Collapsed Nuclei*, *Phys. Rev. D* **4**, 1601 (1971).
- [21] E. Witten, *Cosmic separation of phases*, *Phys. Rev. D* **30**, 272 (1984).
- [22] H. Terazawa, *Super-Hypernuclei in the Quark-Shell Model*, *J. Phys. Soc. Jpn.* **58**, 3555 (1989).
- [23] H. Terazawa, *Super-Hypernuclei in the Quark-Shell Model. II*, *J. Phys. Soc. Jpn.* **58**, 4388 (1989).
- [24] M. Alford, K. Rajagopal, and F. Wilczek, *Color-flavor locking and chiral symmetry breaking in high density QCD*, *Nucl. Phys. B* **537**, 443 (1999).
- [25] M. G. Alford, *Color-Superconducting Quark Matter*, *Ann. Rev. of Nucl. and Part. Phys.* **51**, 131 (2001).
- [26] M. G. Alford et al., *Color superconductivity in dense quark matter*, *Rev. Mod. Phys.* **80**, 1455 (2008).
- [27] G. Lugones and J. E. Horvath, *Color-flavor locked strange matter*, *Phys. Rev. D* **66**, 074017 (2002).
- [28] J. Bardeen, L. N. Cooper, and J. R. Schrieffer, *Microscopic Theory of Superconductivity*, *Phys. Rev.* **106**, 162 (1957).
- [29] J. Bardeen, L. N. Cooper, and J. R. Schrieffer, *Theory of Superconductivity*, *Phys. Rev.* **108**, 1175 (1957).
- [30] P. T. Oikonomou and Ch. C. Moustakidis, *Color-flavor locked quark stars in light of the compact object in the HESS J1731-347 and the GW190814 event*, *Phys. Rev. D* **108**, 063010 (2023).
- [31] M. Alford et al., *Hybrid Stars that Masquerade as Neutron Stars*, *ApJ* **629**, 969 (2005).
- [32] G. Baym et al., *From hadrons to quarks in neutron stars: a review*, *Rep. Prog. Phys.* **81**, 056902 (2018).
- [33] M. G. Alford, S. Han, and M. Prakash, *Generic conditions for stable hybrid stars*, *Phys. Rev. D* **88**, 083013 (2013).
- [34] J. E. Christian, A. Zacchi, and J. Schaffner-Bielich, *Classifications of twin star solutions for a constant speed of sound parameterized equation of state*, *Eur. Phys. J. A* **54**, 28 (2018).
- [35] G. Montaña et al., *Constraining twin stars with GW170817*, *Phys. Rev. D* **99**, 103009 (2019).
- [36] P. S. Koliogiannis and Ch. C. Moustakidis, *Thermodynamical Description of Hot, Rapidly Rotating Neutron Stars, Protoneutron Stars, and Neutron Star Merger Remnants*, *ApJ* **912**, 69 (2021).
- [37] V. Sagun et al., *What Is the Nature of the HESS J1731-347 Compact Object?*, *ApJ* **958**, 49 (2023).
- [38] L. Tsaloukidis et al., *Twin stars as probes of the nuclear equation of state: effects of rotation through the PSR J0952-0607 pulsar and constraints via the tidal deformability from the GW170817 event*, *Phys. Rev. D* **107**, 023012 (2023).
- [39] M. Mariani et al., *Could a slow stable hybrid star explain the central compact object in HESS J1731-347?*, *Phys. Rev. D* **110**, 043026 (2024).
- [40] J. J. Li, A. Sedrakian, and M. Alford, *Hybrid star models in the light of new multi-messenger data*, *ApJ* **967**, 116 (2024).
- [41] P. Laskos-Patkos, P.S. Koliogiannis, and Ch.C. Moustakidis, *Hybrid stars in light of the HESS J1731-347 remnant and the PREX-II experiment*, *Phys. Rev. D* **109**, 063017 (2024).
- [42] X. F. Zhao, *On the moment of inertia of PSR J0348+0432*, *Chin. J. of Phys.* **54**, 839 (2016).
- [43] E. Fonseca et al., *Refined Mass and Geometric Measurements of the High-mass PSR J0740+6620*, *ApJL* **915**, L12 (2021).
- [44] W. R. Romani et al., *PSR J0952-0607: The Fastest and Heaviest Known Galactic Neutron Star*, *ApJL* **934**, L17 (2022).
- [45] B. P. Abbott et al, *GW170817: Measurements of Neutron Star Radii and Equation of State*, *Phys. Rev. Lett.* **121**, 161101 (2018).
- [46] K. Schwarzschild, *On the gravitational field of a mass point according to Einstein's theory*, *Sitzungsber. K. Preuss. Akad. Wiss.*, 189 (1916).
- [47] A. Alho et al., *Compactness bounds in general relativity*, *Phys. Rev. D* **106**, L041502 (2022).
- [48] Ya. B. Zel'dovich, *The equation of state at ultrahigh densities and its relativistic limitations*, *Zh. Eksp. Teoret. Fiz.* **41**, 1609 (1961).
- [49] J. R. Oppenheimer and G. M. Volkoff, *On Massive Neutron Cores*, *Phys. Rev.* **55**, 374 (1939).
- [50] J. Piekarewicz, *Nuclear Astrophysics in the Multimessenger Era: A Partnership Made in Heaven*, *Acta Physica Polonica B* **50**, 239 (2018).
- [51] K. Ch. Chatzisavvas et al., *Complexity and neutron star structure*, *Phys. Lett. A* **373**, 3901 (2009).
- [52] T. DeGrand et al., *Masses and other parameters of the light hadrons*, *Phys. Rev. D* **12**, 2060 (1975).
- [53] C. Vásquez Flores and G. Lugones, *Constraining color flavor locked strange stars in the gravitational wave era*, *Phys. Rev. C* **95**, 025808 (2017).
- [54] S.-H. Yang and C.-M. Pi, *Color-flavor locked strange stars admixed with mirror dark matter and the observations of compact stars*, *JCAP09* **2024**, 052 (2024).